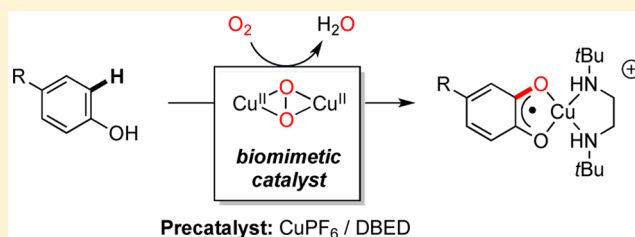


A Biomimetic Mechanism for the Copper-Catalyzed Aerobic Oxygenation of 4-*tert*-ButylphenolMohammad S. Askari,<sup>†</sup> Kenneth Virgel N. Esguerra,<sup>‡</sup> Jean-Philip Lumb,<sup>\*,‡</sup> and Xavier Ottenwaelde<sup>\*,†</sup><sup>†</sup>Department of Chemistry and Biochemistry, Concordia University, Montreal, QC H4B 1R6, Canada<sup>‡</sup>Department of Chemistry, McGill University, Montreal, QC H3A 0B8, Canada

## S Supporting Information

**ABSTRACT:** Controlling product selectivity during the catalytic aerobic oxidation of phenols remains a significant challenge that hinders reaction development. This work provides a mechanistic picture of a Cu-catalyzed, aerobic functionalization of phenols that is selective for phenoxy-coupled *ortho*-quinones. We show that the immediate product of the reaction is a Cu(II)–semiquinone radical complex and reveal that *ortho*-oxygenation precedes oxidative coupling. This complex is the resting state of the Cu catalyst during turnover at room temperature. A mechanistic study of the formation of this complex at low temperatures demonstrates that the oxygenation pathway mimics the dinuclear Cu enzyme tyrosinase by involving a dinuclear side-on peroxodicopper(II) oxidant. Unlike the enzyme, however, the rate-limiting step of the *ortho*-oxygenation reaction is the self-assembly of the oxidant from Cu(I) and O<sub>2</sub>. We provide details for all steps in the cycle and demonstrate that turnover is contingent upon proton-transfer events that are mediated by a slight excess of ligand. Finally, our knowledge of the reaction mechanism can be leveraged to diversify the reaction outcome. Thus, uncoupled *ortho*-quinones are favored in polar, coordinating media, highlighting unusually high levels of chemoselectivity for a catalytic aerobic oxidation of a phenol.



## ■ INTRODUCTION

Selective aerobic oxidations are fundamentally important to the chemical industry due to the abundance of molecular oxygen (O<sub>2</sub>) and the sustainable source of energy provided by its reduction.<sup>1</sup> Despite significant growth in this field, the application of aerobic oxidations to phenols, which are ubiquitous feedstock chemicals, remains underdeveloped due to issues of selectivity.<sup>1b,2</sup> With few exceptions,<sup>3,4</sup> catalytic aerobic oxidations of phenols generate phenoxy radicals that undergo nonselective C–C dimerization or oxidation to the *para*-quinone, limiting their synthetic utility (Scheme 1a).<sup>1b,2</sup> To avoid radical-based reactions, the overwhelming majority of phenolic oxidations used in synthesis employ stoichiometric amounts of a terminal oxidant other than O<sub>2</sub> but do so at the expense of atom- and step-efficiency.<sup>5</sup>

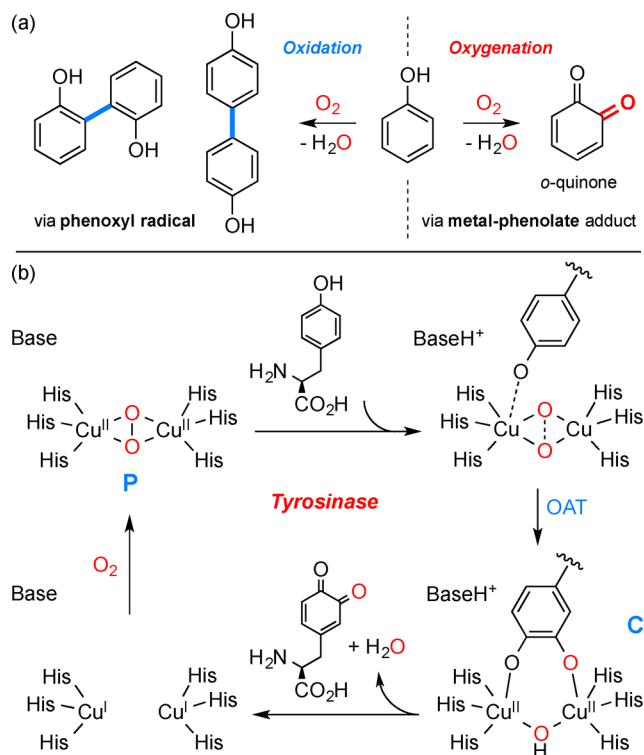
A remarkable example of a selective catalytic aerobic oxygenation of phenols is mediated by the dinuclear Cu enzyme tyrosinase. This enzyme converts L-tyrosine into L-dopaquinone (Scheme 1b) in the first and rate-limiting step of the ubiquitous biosynthesis of melanin pigments.<sup>6</sup> Its fundamental importance for life and its unique reactivity have made tyrosinase the focal point of mechanistic investigations and biomimicry, which have provided considerable insight into factors that govern selectivity in the aerobic oxidation of phenols.<sup>7</sup> More generally, these studies have been fundamentally important in elucidating the speciation of Cu(I) and O<sub>2</sub> in the presence of a vast array of amine ligands.<sup>8</sup> Of particular relevance to tyrosinase and melanogenesis are synthetic mimics

of the enzyme's active site that recreate the characteristic  $\mu$ - $\eta^2$ : $\eta^2$ -peroxodicopper(II) oxidant (P, Scheme 1b). Upon exposure to stoichiometric quantities of sodium, lithium, or tetrabutylammonium phenolate salts, these complexes achieve *ortho*-oxygenation, with the proposed catecholodicopper(II) complex C as the reaction's end point. This leads to catechols or quinones after acidic workup.<sup>9–12</sup> If neutral phenols are used instead of phenolates, *ortho*-oxygenation is not observed, and products of C–C coupling predominate,<sup>11f,13</sup> except in one recent intramolecular case.<sup>14</sup> This has led to the generally accepted view that deprotonation of the phenol must precede the formation of a discrete Cu-phenolate complex, which ensures selective oxygen-atom transfer (OAT) via an inner-sphere mechanism.<sup>4b,15</sup> (In this Article, we use the expression “*ortho*-oxygenation” for the bulk reaction and “OAT” for the specific mechanistic step where the oxygen atom is transferred to the substrate.) Likewise, deprotonation of the phenol substrate is believed to occur during the *ortho*-oxygenation by tyrosinase, where the suitable base is either a histidine residue or an activated water or hydroxide molecule near the enzyme's active site.<sup>7a,16</sup>

The requirement of a phenolate in order to achieve selective OAT has prompted several groups to employ triethylamine (Et<sub>3</sub>N, 2 equiv per substrate) as a buffer for catalytic reactions starting from the phenol.<sup>8c,10e,h,12b,17</sup> Deprotonation of the

Received: June 9, 2015

**Scheme 1. (a) Selectivity Issues upon Oxidation/Oxygenation of Phenols and (b) Simplified Mechanism of the *o*-Oxygenation of L-Tyrosine by Tyrosinase during Melanogenesis<sup>a</sup>**

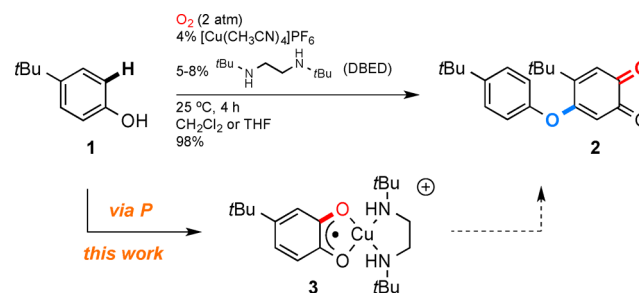


<sup>a</sup>Key:  $\mu$ - $\eta^2$ : $\eta^2$ -peroxodicopper(II) (P) and  $\mu$ -catecholato- $\mu$ -hydroxidicopper(II) (C) intermediates. The nature of the base in the active site is still debated.

phenol in situ affords the necessary phenolate for oxygenation, along with the conjugate acid Et<sub>3</sub>NH<sup>+</sup>, which is thought to be suitably acidic to protonate C. Drawing mechanistic conclusions under these reaction conditions is complicated, however, because of a pronounced background oxygenation of the phenol with Et<sub>3</sub>N, Cu, and O<sub>2</sub> alone (i.e., catalytic oxygenation is observed in the absence of a biomimetic ligand).<sup>4a,b</sup> Since these previous examples have not demonstrated that a P species can form in the presence of Et<sub>3</sub>N and a phenol, it is unclear to what extent independent characterization of P<sup>10c,h,17c,d</sup> relates to catalytic conditions in which P must self-assemble in the presence of all reaction components. Moreover, previous catalytic systems, whether Et<sub>3</sub>N- or phenolate<sup>17e</sup>-based, produce more than one product or do not proceed to complete substrate conversion, which interferes with a mechanistic analysis.

In 2014, one of our groups reported a catalytic aerobic *ortho*-oxygenation of phenols that addresses many of these complications.<sup>4a</sup> It is catalytic in all components, uses a single amine to adjust the reaction pH and ligate Cu, and provides a single product at complete conversion. Thus, oxidation of 4-*tert*-butylphenol, **1**, in the presence of 4 mol % of [Cu(CH<sub>3</sub>CN)<sub>4</sub>](PF<sub>6</sub>) (CuPF<sub>6</sub>) and 5–8 mol % of *N,N'*-di-*tert*-butylethylenediamine (DBED) affords coupled *ortho*-quinone **2** in isolated yields greater than 95% on a multigram scale (Scheme 2). This uniquely simple set of conditions, wherein a single amine additive is used to mediate both O<sub>2</sub> activation and proton transfer, is ideal for mechanistic investigations. This

**Scheme 2. This Paper's Study**



catalytic system finds origin in the stoichiometric experiments of Mirica, Stack, and Solomon (Scheme S1a), whose mechanistic investigations on the *ortho*-oxygenation of 2,4-di-*tert*-butylphenolate provide important spectroscopic signatures of the intermediates involved in O<sub>2</sub> activation and OAT when DBED is used as the ligand.<sup>9,18</sup> In spite of this precedent, the relevance of these intermediates to a catalytic transformation that employs a phenol, as opposed to a phenolate, is unproven (see Scheme S1 for details). Herein, we bridge the gap between stoichiometric experiments and catalytic conditions and provide spectroscopic and kinetic support for a tyrosinase-like mechanism under conditions that are relevant to catalysis.

## RESULTS AND DISCUSSION

**Fast Oxygenation to a Cu(II)–Semiquinone.** At the outset of our work, we monitored the conversion of **1** into **2** by in situ UV–visible spectroscopy. Thus, introduction of O<sub>2</sub> into a CH<sub>2</sub>Cl<sub>2</sub> mixture composed of **1**, 4% CuPF<sub>6</sub>, and 8% DBED at 25 °C<sup>4a</sup> results in the rapid formation of the purple DBED–Cu(II)–semiquinone radical complex **3** ( $\lambda_{\text{max}} = 545 \text{ nm}$ ) along with the product *ortho*-quinone **2** ( $\lambda_{\text{max}} = 426 \text{ nm}$ ) (Figure 1).

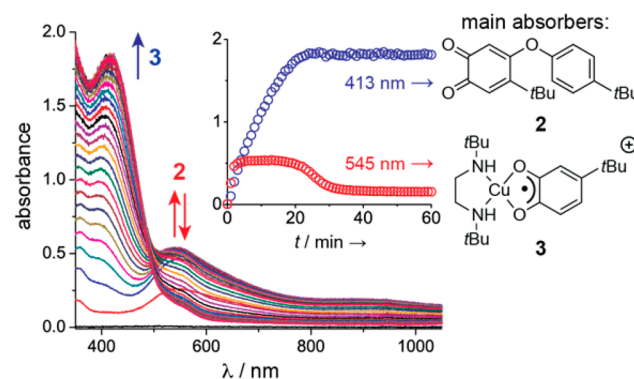


**Figure 1.** In situ UV–vis spectroscopic monitoring under catalytic conditions: CH<sub>2</sub>Cl<sub>2</sub>, 25 °C, 30.7 mM **1**, 4% CuPF<sub>6</sub>, 8% DBED, 1.0 mm path length. Inset: time profiles of the absorbances at 413 and 545 nm, with main absorbing species at these wavelengths.

The structure of **3** was confirmed by an independent synthesis,<sup>19</sup> mass spectrometry, and X-ray crystallography (Figures S1–S4, Supporting Information). Complex **3** remains at a near-steady-state concentration (>95% of the total [Cu]) as long as the reaction turns over to form **2** (Figure 1a, inset).

Time profiling of all species in solution during turnover reveals that the formation of complex **3** is the fastest observable process at room temperature (Figure 2). A small amount of uncoupled 4-*tert*-butyl-*ortho*-quinone **4** is observed along with **3** and remains at a concentration of  $\sim 9\%$  of [**1**]<sub>0</sub> throughout

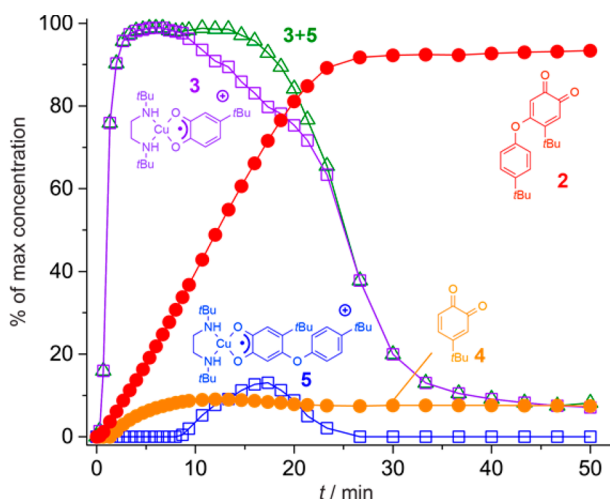
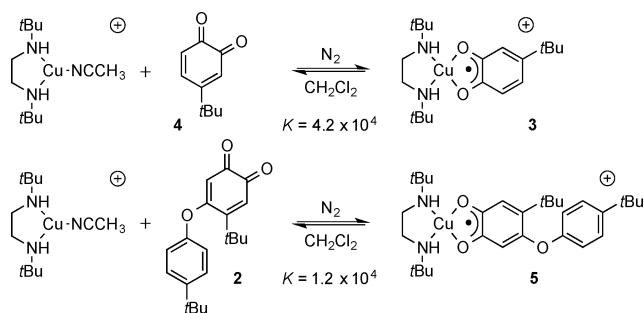


**Figure 2.** Concentrations of absorbing species during the reaction of Figure 1, deduced by fitting UV-vis spectra at various time points (e.g., Figure S3). The y-axis is scaled to the maximum concentration of each species, i.e.,  $[3]_{\max} = [5]_{\max} = [\text{CuPF}_6]_0$ ,  $[4]_{\max} = [1]_0$ , and  $[2]_{\max} = 0.5[1]_0$ . Thus, each point in the graph gives the yield of each species.

turnover (Figure 2).<sup>20</sup> As the concentration of 2 increases, its corresponding Cu(II)–semiquinone complex 5 is observed. Quinones 2 and 4 are in equilibrium with their Cu(II)–semiquinone complexes, 3 and 5, respectively, with stronger binding observed between DBED–Cu(I) and the more electron-deficient quinone 4 (Scheme 3 and Figures S5 and

**Scheme 3.** DBEDCu(I)–Quinone Binding Constants<sup>a</sup>



<sup>a</sup>The Cu(I) complex was prepared by mixing DBED and  $[\text{Cu}(\text{CH}_3\text{CN})_4](\text{PF}_6)_2$  in a 1:1 ratio. Thus, a total of 4 equiv of  $\text{CH}_3\text{CN}$  is present in solution.

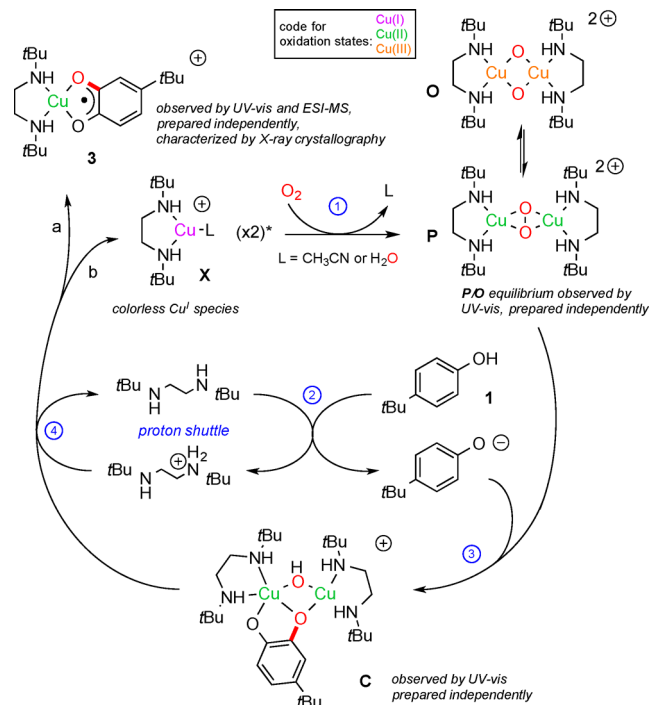
S6). Complex 3 is the predominant Cu species until the concentration of 2 approaches 50%, at which point the concentration of complex 5 grows. Subsequent decay of 5 (and 3) is consistent with its dissociation and subsequent oxidation of DBED–Cu(I) to the spectrally innocuous bis( $\mu$ -hydroxo)dicopper(II) complex,<sup>21</sup> which does not re-coordinate the quinones. We have previously demonstrated that this Cu(II)–hydroxide dimer can re-enter the catalytic cycle, such that its formation does not preclude catalysis.<sup>4c</sup>

The conversion of 3 into 2 is the rate-limiting sequence of the reaction at 25 °C, and it does not proceed at –78 °C. When the reaction is run at –78 °C, 3 is the only visible species, and it forms quantitatively with respect to the starting amount of Cu. Upon warming to 25 °C, turnover proceeds and 2 forms in 96% NMR yield, indicating that 3 is a competent intermediate. Complex 3 is also a suitable precatalyst for the reaction, as

evidenced by the complete conversion of 1 to 2 when 5 mol % of 3 is used as the only source of Cu, along with an additional 5 mol % of DBED.

**Mechanistic Proposal for the *ortho*-Oxygenation.** The selective formation of Cu(II)–semiquinone 3 from phenol 1 at low temperatures enabled us to study the mechanism of *ortho*-oxygenation in the absence of the oxidative coupling. A plausible mechanism for this transformation at –80 °C is provided in Scheme 4 and forms the basis for the ensuing discussion.

**Scheme 4.** Proposed Mechanism for the *o*-Oxygenation of Phenol 1 to Cu(II)–Semiquinone Complex 3 at –80 °C



\*Step 4 produces one molecule of a Cu(I) complex, but two are required in step 1.

**Kinetic Measurements and Isotopic Labeling.** To probe the initial stages of the mechanism, the formation of 3 was analyzed using stopped-flow kinetic experiments at –80 °C. The initial rate of the reaction shows a second-order dependence on  $[\text{CuPF}_6]$  (Figures 3 and S10), which is consistent with the two-step formation of a dinuclear species,

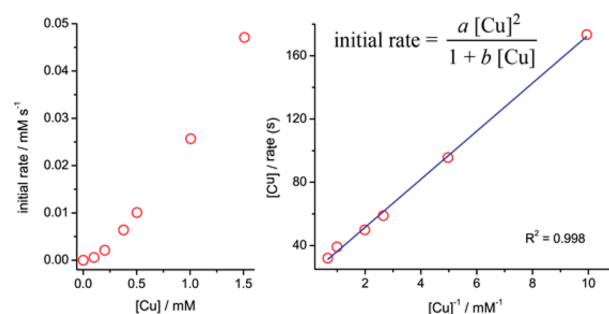
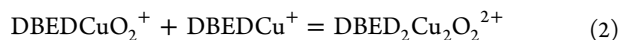


**Figure 3.** Dependence of the initial rate of formation of 3 on  $[\text{CuPF}_6]$  = 0.1–1.5 mM,  $[1] = 2.5$  mM,  $[\text{DBED}]/[\text{CuPF}_6] = 1.1$  in  $\text{CH}_2\text{Cl}_2$  at –80 °C.



as expressed in eqs 1 and 2.<sup>22</sup> This provides the first kinetic support for a dinuclear mechanism of O<sub>2</sub> activation under biomimetic *ortho*-oxygenation conditions.



The substrate does not participate in the rate-limiting step of the reaction. With a [DBED]/[CuPF<sub>6</sub>] ratio maintained at 1.1, no significant changes in the initial rate were observed upon varying [1] (Figure S12), suggesting a zeroth order dependence on substrate concentration. This result is consistent with the absence of a kinetic isotope effect (KIE) when isotopically labeled 4-*tert*-butyl-2-deuterophenol (1<sup>HD</sup>) or 4-*tert*-butyl-2,6-dideuterophenol (1<sup>DD</sup>) is used instead of 1 (Figure S13). These results create an important distinction with Mirica's stoichiometric experiments using a preformed P species and suggest that the rate of self-assembly of the dinuclear Cu oxidant (O<sub>2</sub> activation) is rate-determining under catalytically relevant conditions at −80 °C.

The OAT event that converts 1 into 3 was probed via product analysis in the −78 °C reaction of 1<sup>HD</sup>, where competition is present between a C–H and a C–D bond at the *ortho* positions of the phenol (Table S2). In this case, we observed an intrinsic KIE of 0.87(3), which is consistent with previously reported values using tyrosinase<sup>23</sup> or synthetic mimics<sup>6d,24</sup> and supports a mechanism of C–O bond formation via electrophilic aromatic substitution. Following OAT, a fast proton migration of the *ortho* H/D atom aromatizes the substrate and leads to bridged catecholate C, in line with previous mechanistic hypotheses (e.g., Scheme 1b; see below for additional discussion).

**Intermediates in the Oxygenation.** The second-order dependence in Cu supports a dinuclear mechanism for O<sub>2</sub> activation that is consistent with the mechanism of tyrosinase and previous work by Mirica, Stack, and Solomon with the DBED ligand (Scheme S1a).<sup>9</sup> To gain insight into the structures of the key dinuclear intermediates, we monitored the oxygenation of a solution composed of 1, 4% CuPF<sub>6</sub>, and 5% DBED at −115 °C in 2-methyltetrahydrofuran (MeTHF). This generates a solution with an intense feature at 353 nm, possessing a small shoulder at 418 nm (Figure 4i–ii, and Figure S8).<sup>8a</sup> The same spectral features are observed upon the oxygenation of a 1:1 mixture of CuPF<sub>6</sub> and DBED in the absence of phenol (Figure S9),<sup>18</sup> indicating the formation of a ~5:1 mixture of rapidly interconverting<sup>8a</sup> P and O species.<sup>26</sup> Within minutes, the reaction, which contains phenol and a small excess of DBED per Cu, evolves to a 1:4 mixture of 3 and a species we tentatively assign as a catecholathydroxodicopper(II) complex, C (λ<sub>max</sub> = 800 nm, Figure 4iii and Figure S10).<sup>9b</sup> The assignment of C is supported by its independent synthesis from preformed P and 2.5 equiv of 4-*tert*-butylphenolate according to literature.<sup>9b</sup> The UV–visible spectrum of the obtained species is comparable to that reported by Mirica et al. with 2,4-di-*tert*-butylphenolate (Figure 5iii and Figure S10)<sup>27</sup> and so is its reactivity (release of 3 upon addition of 2.5 equiv of H<sup>+</sup> from H<sub>2</sub>SO<sub>4</sub>).

Upon subsequent warming to −78 °C, the reaction mixture affords 3 in >90% yield with respect to the starting amount of CuPF<sub>6</sub> (Figure 4iv). This percentage proves that the spectroscopically silent Cu species that forms upon cleavage of dinuclear C to mononuclear 3 can re-enter the oxygenation cycle to form additional 3 (details below). Since the

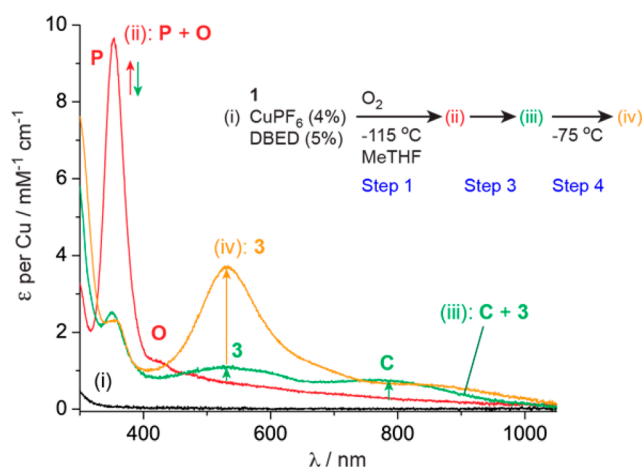


**Figure 4.** Intermediates in the oxygenation of 1 to 3. Oxygenation at −115 °C of a MeTHF solution containing 1 (24.85 mM), 4% CuPF<sub>6</sub>, and 5% DBED. (i, black) Solution before introducing O<sub>2</sub>. (ii, red) Spectrum after oxygenating for 3 min, indicating the presence of P and O. (iii, green) Spectrum after 91 min under O<sub>2</sub>, indicating a ~4:1 mixture of C (800 nm) and 3 (545 and 900 nm). (iv, orange) Warming up to −78 °C under O<sub>2</sub> shows the conversion of C to >90% 3.

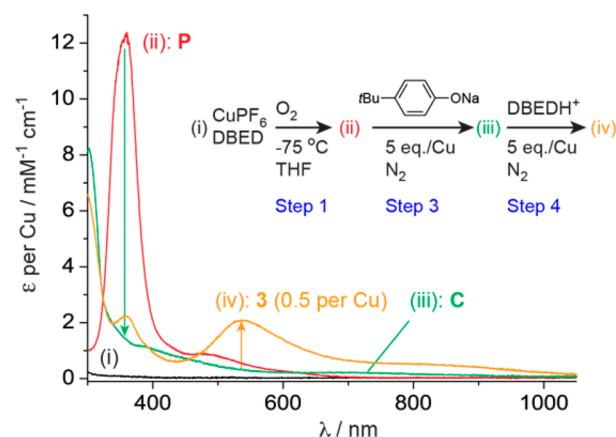


**Figure 5.** Closing the catalytic cycle: cleavage of C. P is formed by oxygenating a 1:1 solution of DBED/CuPF<sub>6</sub> in THF at −78 °C (i → ii). Addition 2.51 equiv of sodium 4-*tert*-butylphenolate (per P) under N<sub>2</sub> leads to the formation of C (iii). Addition of 2.54 equiv of DBEDH(PF<sub>6</sub>) forms 1 equiv of 3 with respect to P (iv). More details are provided in the Supporting Information.

dissociation of C occurs rapidly at −78 °C, 3 forms quantitatively relative to the total Cu concentration.

The P, C, and 3 intermediates are analogous to those observed under Mirica's stoichiometric experiments, but the absence of a visible intermediate between P and C is an important distinction. Whereas Mirica et al. observed a transient bis(oxo)phenolato complex A upon addition of 2,4-di-*tert*-butylphenolate to P at −115 °C (Scheme S1),<sup>9b</sup> we do not observe an A species under our catalytically relevant conditions (Figure 4i→iii). An A species is also absent when the oxygenation of 1 is performed using its sodium phenolate under conditions identical to those reported by Mirica (Figure Sii→iii). We attribute this difference to a much faster OAT when the starting phenol lacks a 2-*tert*-butyl substituent.

**Protonation of C and Catalyst Regeneration.** The key step that enables catalyst turnover is the cleavage of C to 3 by

redox tautomerization of the catecholate and the two Cu(II) centers of the dinuclear complex. Since this process is triggered by protonation of the hydroxide bridge,<sup>9b</sup> stoichiometric oxidations using phenolate salts cannot close the catalytic cycle of *ortho*-oxygenation. Under catalytic conditions, deprotonation of neutral phenol **1** by uncoordinated DBED (DBED is in excess of Cu) affords the mild acid DBEDH<sup>+</sup>. DBEDH<sup>+</sup> is a suitably strong acid to protonate **C** and release **3** along with a colorless Cu(I) species that is capable of re-entering the *ortho*-oxygenation cycle. We demonstrate this explicitly by the synthesis of **C** from **P** and the sodium phenolate of **1** at  $-78\text{ }^{\circ}\text{C}$  (Figure Siii). Subsequent addition of DBEDH(PF<sub>6</sub>) (prepared separately) affords 1 equiv of mononuclear **3** per dinuclear **C** (Figure Siv), along with a Cu-containing species, **X**, which is spectroscopically silent. Species **X** can re-enter the oxygenation cycle, as demonstrated in Figure 6. Thus, the reaction of **1** (2 equiv) with preformed **P**

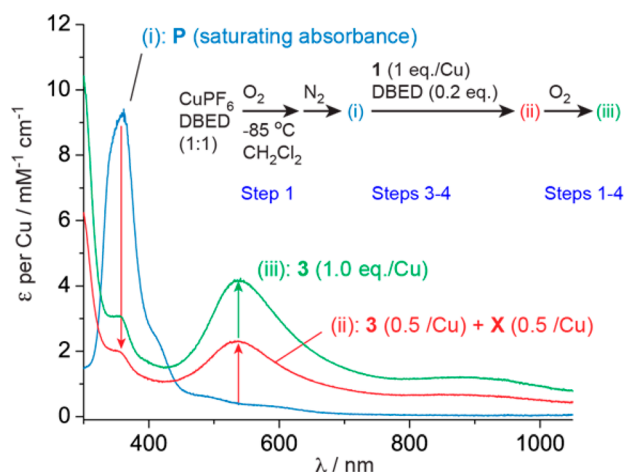


**Figure 6.** Closing the catalytic cycle: fate of the released Cu. (i) **P** species  $-85\text{ }^{\circ}\text{C}$  in  $\text{CH}_2\text{Cl}_2$  under  $\text{N}_2$ . (ii) Addition of **1** and a catalytic amount of DBED rapidly forms **3** (56% of the total [Cu]). (iii) After  $\text{O}_2$  is reintroduced, **3** grows to 100% of the total [Cu]. More details are provided in the Supporting Information.

(1 equiv) under  $\text{N}_2$  at  $-85\text{ }^{\circ}\text{C}$  in the presence of a catalytic quantity of DBED (20% per Cu) rapidly forms 1 equiv of **3** from every starting **P** (Figure 6ii). If  $\text{O}_2$  is introduced at this point, all remaining Cu present in solution is rapidly converted into **3** (Figure 6iii), confirming that **X** is suitable for additional turnover to **3**. The demonstration that **X** promotes additional conversion of **1** into **3** closes the cycle of *ortho*-oxygenation and provides an explicit demonstration that the cleavage of **C** releases a catalytically competent Cu species.<sup>10e</sup>

**Discussion on the Mechanism.** The visualization of **P** in the presence of a large excess of phenol under conditions that retain selectivity for *ortho*-oxygenation is noteworthy since **P** species are known to react with phenols via radical-based pathways.<sup>13</sup> In the absence of a small excess of DBED with respect to  $\text{CuPF}_6$ , preformed **P** does not react with **1** at  $-80\text{ }^{\circ}\text{C}$ , and **1** is recovered after workup, as is the case with 2,4-*tert*-butylphenol.<sup>18</sup> This strongly suggests that the *ortho*-oxygenation must proceed through the phenolate and underscores the importance of a slight excess of DBED per Cu for turnover. Consistent with the second-order dependence of the rate on  $[\text{CuPF}_6]$ ,<sup>22</sup> our mechanistic proposal at  $-80\text{ }^{\circ}\text{C}$  (Scheme 4) begins by assembling **P** from DBED–Cu(I) and  $\text{O}_2$  (step 1), which then reacts with the in situ generated

phenolate to make **C** (steps 2 and 3). Protonation of dicopper species **C** by DBEDH<sup>+</sup> releases **3** and Cu(I) complex **X**, which re-enters the oxygenation cycle (step 4). At  $-78\text{ }^{\circ}\text{C}$ , complex **3** is kinetically inert and requires higher temperatures to oxidatively couple with **1** to afford **2**. Upon formation of the more electron-rich quinone **2**, DBED–Cu(I) is more easily released from the intermediate semiquinone **5** and can either re-enter the catalytic cycle or oxidize to the bis( $\mu$ -hydroxo)-dicopper(II) species.

The absence of a KIE between **1** and **1**<sup>DD</sup> and the zeroth order dependence on  $[\text{I}]$  indicate that the OAT step is not rate-limiting at  $-80\text{ }^{\circ}\text{C}$ . Instead, the rate of *ortho*-oxygenation is dependent on the formation of **P**, which requires the self-assembly of  $\text{O}_2$  and two molecules of DBED–Cu(I). This is distinct from the oxygenation of phenols catalyzed by tyrosinase, which rapidly forms **P** due to the colocalization of the two Cu(I) centers. The inverse intramolecular isotopic effect observed with **1**<sup>HD</sup> (0.87) is consistent with an electrophilic aromatic substitution being the product-determining step. Whether OAT proceeds via a discrete Cu–phenolate species like **A** or by direct attack of the electron-rich aromatic ring onto the oxygen atom of **P** remains unclear, but efforts are underway to distinguish between these two possibilities.

**Diverting the Course of the Dearomatization Reaction.** The involvement of **3** in the formation of coupled *ortho*-quinone **2** at higher temperatures ( $25\text{ }^{\circ}\text{C}$ ) creates an opportunity to divert the course of the reaction to uncoupled *ortho*-quinone **4** by simply changing the solvent from  $\text{CH}_2\text{Cl}_2$  to acetonitrile ( $\text{CH}_3\text{CN}$ ). The coordinating ability of  $\text{CH}_3\text{CN}$  can reverse the equilibrium position between **3** and **4** (Scheme 3) in favor of **4** (Figure S7). Thus, conducting the catalytic reaction in pure  $\text{CH}_3\text{CN}$  affords a 1:1 mixture of quinones **2** and **4** at  $25\text{ }^{\circ}\text{C}$  (Table 1, entry 2) and a 1:4 mixture at  $-40\text{ }^{\circ}\text{C}$

**Table 1.** Diversification of the Reaction Outcome<sup>a</sup>

entry	$\text{CuPF}_6$ (mol %)	DBED (mol %)	solvent	$T\text{ (}^{\circ}\text{C)}$	yield (%) <sup>b</sup>		
					<b>2</b>	<b>4</b>	<b>6</b>
1 <sup>c</sup>	4	8	$\text{CH}_2\text{Cl}_2$	25	98	0	0
2 <sup>c</sup>	4	8	$\text{CH}_3\text{CN}$	25	52	47	0
3 <sup>c</sup>	4	8	$\text{CH}_3\text{CN}$	$-40$	18	76	0
4 <sup>c</sup>	100	110	$\text{CH}_2\text{Cl}_2$	$-78$	0	82	0
5 <sup>d</sup>	100	110	$\text{CH}_2\text{Cl}_2$	$-78$	0	0	81

<sup>a</sup>Reactions performed on 1 mmol of phenol. <sup>b</sup>Isolated yields. <sup>c</sup>Workup with 10%  $\text{NaHSO}_4$ . <sup>d</sup>Saturated  $\text{Na}_2\text{S}_2\text{O}_4$  workup. See Supporting Information for experimental details.

(entry 3). Under these conditions, we do not observe **3** by UV–visible spectroscopy, which suggests that  $\text{CH}_3\text{CN}$  coordination to Cu(I) promotes the release of **4** faster than oxidative coupling with **1** to afford **2**. This scenario constitutes an important proof of principle that the *ortho*-oxygenation reaction can be performed in isolation of oxidative coupling, which is attractive for synthetic applications.

If complete selectivity for **4** is desired, the oxygenation of **1** can be carried out at  $-78\text{ }^{\circ}\text{C}$  in  $\text{CH}_2\text{Cl}_2$  with 1 equiv of  $\text{CuPF}_6$  and 1.1 equiv of DBED, which results in the quantitative

formation of **3**. Subsequent exposure of **3** to either acidic or reductive conditions affords uncoupled *ortho*-quinone **4** (entry 4) or catechol **6** (entry 5), respectively. Semiquinones related to **3** have been popularized as noninnocent ligands for late transition metals,<sup>28</sup> but they have not been explored as strategic intermediates for synthesis. To our knowledge, this is the first synthesis of a semiquinone–metal complex directly from a phenol—these complexes are typically formed by inner-sphere reaction between a low-valent metal and an *ortho*-quinone.<sup>28</sup> This is also the first illustration that semiquinone–metal complexes are viable precursors to either free *ortho*-quinones or catechols, setting the stage for their development into strategic intermediates for synthesis.

## CONCLUSIONS

Building upon the stoichiometric studies by Mirica, Solomon, and Stack,<sup>9</sup> we establish that (1) the tyrosinase-like **P** species is indeed a viable oxidant under catalytic conditions and in the presence of excess phenol, (2) *ortho*-oxygenation under catalytic conditions requires deprotonation of the phenol, and (3) DBED is a suitable buffer to mediate proton transfer between **1** and **C**. In this sense, the *ortho*-oxygenation pathway under DBED/CuPF<sub>6</sub> conditions is very similar to that of tyrosinase, which proceeds through a **P** species, exhibits phenol deprotonation, and requires protonation of **C** for substrate release.<sup>6,7</sup> However, the formation of Cu(II)–semiquinone **3** marks an important point of divergence from tyrosinase. In the enzyme, both Cu atoms are retained in the protein-constrained active site following *ortho*-oxygenation.<sup>6a,d,7a</sup> This constraint enforces the release of the relatively unstable L-dopaquinone, which is prone to polymerization.<sup>29</sup> By contrast, our reaction attenuates the reactivity of the *ortho*-quinone by keeping it bound to Cu as a partially reduced semiquinone radical. Our work marks an important extension of mechanistic data acquired under stoichiometric conditions at cryogenic temperatures to a catalytic transformation that is conducted at room temperature on a gram scale. This provides a mechanistic framework from which to explore the aerobic dearomatization of phenols, a reaction that holds significant promise for synthesis, but for which few selective catalytic aerobic systems have been developed.

## EXPERIMENTAL SECTION

Chemicals and solvents were purchased from Sigma-Aldrich, Alfa Aesar, or Strem Chemicals. Inhibitor-free solvents were dried using a MBraun SPS 800, transferred to an inert-atmosphere glovebox (MBraun Labmaster, <1 ppm of O<sub>2</sub> and H<sub>2</sub>O, filled with a dry N<sub>2</sub> atmosphere), further degassed under vacuum, and stored over activated molecular sieves (4 Å). *tert*-Butylphenol **1** was purified by double recrystallization from CH<sub>2</sub>Cl<sub>2</sub>/hexanes. *N,N'*-Di-*tert*-butylethylenediamine (DBED) was distilled over CaH<sub>2</sub> under N<sub>2</sub> and stored in the glovebox. The copper(I) salt [Cu(CH<sub>3</sub>CN)<sub>4</sub>](PF<sub>6</sub>), abbreviated CuPF<sub>6</sub>, was purchased from commercial sources or made via a literature procedure.<sup>30</sup> [Cu(CH<sub>3</sub>CN)<sub>4</sub>](SbF<sub>6</sub>) was prepared via the same method but using HSbF<sub>6</sub> instead of HPF<sub>6</sub>. All copper(I) complexes were stored inside the glovebox.

Unless otherwise noted, reactions were performed in oven-dried glassware under a positive pressure of nitrogen using standard synthetic inert-atmosphere techniques. Bulk oxidation reactions were setup in the glovebox in 25-mL Radley tubes equipped with a Teflon-coated stir bar. The reaction vessels were then connected to a cylinder of O<sub>2</sub>, purged three times with O<sub>2</sub>, and then overpressurized to +1.0 atm.

UV–visible spectra were recorded on a B&W Tek iTrometer equipped with fiber-optic cables connected to a Hellma full-quartz dip-

probe having a 1.0 mm path length. The probe was immersed in the solution inside a custom-made Schlenk flask. Temperature was maintained with external cooling baths: acetone/dry ice (−75 °C inside the solution), acetone/liquid nitrogen (−85 °C), pentane/liquid nitrogen (−115 °C). Spectra for mixtures or evolving solutions are reported in apparent  $\epsilon$ , that is, molar extinction coefficients with respect to the total Cu concentration.

Low-temperature stopped-flow experiments were carried out in the Département de Chimie at the Université de Montréal on a Hi-Tech CSF-61DX2 instrument (TgK Scientific) equipped with a diode-array detector over the 300–700 nm range. The UV–vis cuvette (pathlengths of 1.5 or 10 mm) was cooled by immersion in an ethanol bath cooled with liquid N<sub>2</sub>. Syringe 1 was filled with a CH<sub>2</sub>Cl<sub>2</sub> solution containing **1**, DBED, and CuPF<sub>6</sub> in desired concentrations that was prepared in an MBraun Labmaster glovebox. Syringe 2 was filled with CH<sub>2</sub>Cl<sub>2</sub> that was O<sub>2</sub>-saturated at atmospheric pressure and room temperature. Concentrations were corrected for the 2-fold dilution upon mixing. Initial rates were calculated by measuring the tangent of the growth of the absorbance at 545 nm at the initial stage of the reaction (150 ms after mixing) and using  $\epsilon_{545}(\mathbf{3}) = 4100 \text{ M}^{-1} \text{ cm}^{-1}$ .

Intramolecular competition experiments on **1**<sup>HD</sup> were carried out on solutions containing 52 mM **1**<sup>HD</sup>, 52 mM CuPF<sub>6</sub>, and 58 mM DBED in CH<sub>2</sub>Cl<sub>2</sub> at −78 °C under 2 atm O<sub>2</sub> for 4 h. Reductive workup with Na<sub>2</sub>S<sub>2</sub>O<sub>4</sub> yielded the catechols. The ratios of **6** (major) to 5-*tert*-butyl-3-deuterocatechol (**6**<sup>D</sup>, minor) were measured by GC-MS on an Agilent 7890A GC with a HP 140915-433A column and an Agilent 5975C VL MSD (EI, 70 eV). Details are in Table S2.

**Independent synthesis of **3**.**<sup>19</sup> **3**(PF<sub>6</sub>): To a solution of DBED (51.8 mg, 0.30 mmol, 1.1 equiv) and CuPF<sub>6</sub> (100 mg, 0.27 mmol, 1 equiv) in 4 mL of THF was added a solution of 4-*tert*-butylquinone (**4**, 48.5 mg, 0.30 mmol, 1.1 equiv) in 1 mL of THF with stirring. The color of the solution immediately changed from light pink to deep purple. The solution was stirred for 2 h at 25 °C under N<sub>2</sub>. The solution was then filtered through Celite and added to 15 mL of stirring pentane precooled to −35 °C, upon which a purple solid precipitated. The solid was collected, washed with 2 mL of Et<sub>2</sub>O and 2 × 2 mL of pentane, and dried under vacuum for 24 h. Yield: 110 mg, 75%. UV–vis, CH<sub>2</sub>Cl<sub>2</sub>, 25 °C,  $\lambda/\text{nm}$  ( $\epsilon/\text{M}^{-1} \text{ cm}^{-1}$ ): 230 (6,380), 300 (9,000), 359 (1,910), 545 (3,500), 915 (1,300). Elemental analysis (mol %): expected for C<sub>20</sub>H<sub>36</sub>N<sub>2</sub>O<sub>2</sub>F<sub>6</sub>PCu·0.9CH<sub>3</sub>CN·1.8H<sub>2</sub>O: C, 42.62; H, 6.94; N, 6.61; found C, 42.75; H, 6.90; N, 6.61. Structural analysis of weakly diffracting crystals showed the same structure as that for the **3**(SbF<sub>6</sub>) structure below, with the exception of smaller unit cell dimensions and a disordered PF<sub>6</sub><sup>−</sup> instead of SbF<sub>6</sub><sup>−</sup>.

**3**(SbF<sub>6</sub>): This compound was prepared similarly using [Cu(CH<sub>3</sub>CN)<sub>4</sub>](SbF<sub>6</sub>) as the copper source. Crystals suitable for X-ray diffraction studies were grown by slow layered diffusion of pentane into a CH<sub>2</sub>Cl<sub>2</sub> solution of the complex at −30 °C in the glovebox. **3**(SbF<sub>6</sub>) was only used for structural characterization. For all solution experiments, the PF<sub>6</sub><sup>−</sup> salt was used.

## ASSOCIATED CONTENT

### Supporting Information

The Supporting Information is available free of charge on the ACS Publications website at DOI: 10.1021/acs.inorgchem.5b01297.

X-ray data for **3** (CCDC-950162) (CIF)

Experimental and kinetic details, spectroscopic characterization of intermediates (PDF)

## AUTHOR INFORMATION

### Corresponding Authors

\*E-mail: jean-philip.lumb@mcgill.ca.

\*E-mail: dr.x@concordia.ca.



## Funding

Financial support was provided by the Natural Sciences and Engineering Council of Canada, the Fonds de Recherche du Québec–Nature et Technologies and the Centre de Chimie Verte et Catalyse (Quebec).

## Notes

The authors declare no competing financial interest.

## ACKNOWLEDGMENTS

We are grateful to Prof. Hein Schaper and Prof. Garry Hanan (Université de Montréal) for access to their cryo-stopped-flow and glovebox equipment. M.S.A. acknowledges NSERC for a PGS-D scholarship.

## REFERENCES

- (1) (a) Punniyamurthy, T.; Velusamy, S.; Iqbal, J. *Chem. Rev.* **2005**, *105*, 2329–2364. (b) Allen, S. E.; Walvoord, R. R.; Padilla-Salinas, R.; Kozłowski, M. C. *Chem. Rev.* **2013**, *113*, 6234–6458. (c) Wendlandt, A. E.; Suess, A. M.; Stahl, S. S. *Angew. Chem., Int. Ed.* **2011**, *50*, 11062–11087. (d) Que, L.; Tolman, W. B. *Nature* **2008**, *455*, 333–340. (e) Piera, J.; Bäckvall, J.-E. *Angew. Chem., Int. Ed.* **2008**, *47*, 3506–3523.
- (2) (a) Yamamura, S. *The Chemistry of Phenols*; John Wiley & Sons, Ltd.: West Sussex, U.K., 2003. (b) Quideau, S.; Deffieux, D.; Pouységu, L. *Comprehensive Organic Synthesis II*, 2nd ed.; Elsevier: Amsterdam, 2014.
- (3) (a) Hay, A. S.; Blanchard, H. S.; Endres, G. F.; Eustance, J. W. *J. Am. Chem. Soc.* **1959**, *81*, 6335–6336. (b) Endres, G. F.; Hay, A. S.; Eustance, J. W. *J. Org. Chem.* **1963**, *28*, 1300–1305. (c) Hay, A. S. *Polym. Eng. Sci.* **1976**, *16*, 1–10. (d) Lee, Y. E.; Cao, T.; Torruellas, C.; Kozłowski, M. C. *J. Am. Chem. Soc.* **2014**, *136*, 6782–6785.
- (4) (a) Esguerra, K. V. N.; Fall, Y.; Lumb, J.-P. *Angew. Chem., Int. Ed.* **2014**, *53*, 5877–5881. (b) Esguerra, K. V. N.; Fall, Y.; Petitjean, L.; Lumb, J.-P. *J. Am. Chem. Soc.* **2014**, *136*, 7662–7668. (c) Askari, M. S.; Rodriguez-Solano, L. A.; Proppe, A.; McAllister, B.; Lumb, J. P.; Ottenwaelde, X. *Dalton Trans.* **2015**, *44*, 12094–12097.
- (5) (a) Pouységu, L.; Deffieux, D.; Quideau, S. *Tetrahedron* **2010**, *66*, 2235–2261. (b) Quideau, S.; Deffieux, D.; Douat-Casassus, C.; Pouységu, L. *Angew. Chem., Int. Ed.* **2011**, *50*, 586–621. (c) Pouységu, L.; Sylla, T.; Garnier, T.; Rojas, L. B.; Charris, J.; Deffieux, D.; Quideau, S. *Tetrahedron* **2010**, *66*, 5908–5917. (d) Roche, S. P.; Porco, J. A. *Angew. Chem., Int. Ed.* **2011**, *50*, 4068–4093. (e) Magdziak, D.; Rodriguez, A. A.; Van De Water, R. W.; Pettus, T. R. *Org. Lett.* **2002**, *4*, 285–288. (f) Uyanik, M.; Mutsuga, T.; Ishihara, K. *Molecules* **2012**, *17*, 8604–8616.
- (6) (a) Solomon, E. I.; Sundaram, U. M.; Machonkin, T. E. *Chem. Rev.* **1996**, *96*, 2563–2606. (b) Decker, H.; Schweikardt, T.; Tuzcek, F. *Angew. Chem., Int. Ed.* **2006**, *45*, 4546–4550. (c) Fairhead, M.; Thöny-Meyer, L. *New Biotechnol.* **2012**, *29*, 183–191. (d) Solomon, E. I.; Heppner, D. E.; Johnston, E. M.; Ginsbach, J. W.; Cirera, J.; Qayyum, M.; Kieber-Emmons, M. T.; Kjaergaard, C. H.; Hadt, R. G.; Tian, L. *Chem. Rev.* **2014**, *114*, 3659–3853.
- (7) (a) Rolff, M.; Schottenheim, J.; Decker, H.; Tuzcek, F. *Chem. Soc. Rev.* **2011**, *40*, 4077–4098. (b) Hatcher, L. Q.; Karlin, K. D. *Adv. Inorg. Chem.* **2006**, *58*, 131–184.
- (8) (a) Mirica, L. M.; Ottenwaelde, X.; Stack, T. D. P. *Chem. Rev.* **2004**, *104*, 1013–1046. (b) Lewis, E. A.; Tolman, W. B. *Chem. Rev.* **2004**, *104*, 1047–1076. (c) Citek, C.; Herres-Pawlis, S.; Stack, T. D. P. *Acc. Chem. Res.* **2015**, *48*, 2424.
- (9) (a) Mirica, L. M.; Vance, M.; Rudd, D. J.; Hedman, B.; Hodgson, K. O.; Solomon, E. I.; Stack, T. D. P. *Science* **2005**, *308*, 1890–1892. (b) Op't Holt, B. T.; Vance, M. A.; Mirica, L. M.; Heppner, D. E.; Stack, T. D. P.; Solomon, E. I. *J. Am. Chem. Soc.* **2009**, *131*, 6421–6438.
- (10) (a) Santagostini, L.; Gullotti, M.; Monzani, E.; Casella, L.; Dillinger, R.; Tuzcek, F. *Chem. - Eur. J.* **2000**, *6*, 519–522. (b) Itoh, S.; Kumei, H.; Taki, M.; Nagatomo, S.; Kitagawa, T.; Fukuzumi, S. *J. Am. Chem. Soc.* **2001**, *123*, 6708–6709. (c) Battaini, G.; Carolis, M. D.; Monzani, E.; Tuzcek, F.; Casella, L. *Chem. Commun.* **2003**, 726–727. (d) Palavicini, S.; Granata, A.; Monzani, E.; Casella, L. *J. Am. Chem. Soc.* **2005**, *127*, 18031–18036. (e) Rolff, M.; Schottenheim, J.; Peters, G.; Tuzcek, F. *Angew. Chem., Int. Ed.* **2010**, *49*, 6438–6442. (f) Citek, C.; Lyons, C. T.; Wasinger, E. C.; Stack, T. D. P. *Nat. Chem.* **2012**, *4*, 317–322. (g) Matsumoto, J.; Kajita, Y.; Masuda, H. *Eur. J. Inorg. Chem.* **2012**, *2012*, 4149–4158. (h) Hoffmann, A.; Citek, C.; Binder, S.; Goos, A.; Rübhausen, M.; Troeppner, O.; Ivanović-Burmazović, I.; Wasinger, E. C.; Stack, T. D. P.; Herres-Pawlis, S. *Angew. Chem., Int. Ed.* **2013**, *52*, 5398–5401.
- (11) For examples of phenolate oxygenations by well-characterized Cu–O<sub>2</sub> complexes other than P, see: (a) Company, A.; Palavicini, S.; Garcia-Bosch, I.; Mas-Ballesté, R.; Que, L.; Rybak-Akimova, E. V.; Casella, L.; Ribas, X.; Costas, M. *Chem. - Eur. J.* **2008**, *14*, 3535–3538. (b) Herres-Pawlis, S.; Verma, P.; Haase, R.; Kang, P.; Lyons, C. T.; Wasinger, E. C.; Flörke, U.; Henkel, G.; Stack, T. D. P. *J. Am. Chem. Soc.* **2009**, *131*, 1154–1169. (c) Garcia-Bosch, I.; Company, A.; Frisch, J. R.; Torrent-Sucarrat, M.; Cardellach, M.; Gamba, I.; Güell, M.; Casella, L.; Que, L.; Ribas, X.; Luis, J. M.; Costas, M. *Angew. Chem., Int. Ed.* **2010**, *49*, 2406–2409. (d) Mandal, S.; Mukherjee, J.; Lloret, F.; Mukherjee, R. *Inorg. Chem.* **2012**, *51*, 13148–13161. (e) Garcia-Bosch, I.; Ribas, X.; Costas, M. *Chem. - Eur. J.* **2012**, *18*, 2113–2122. (f) Serrano-Plana, J.; Garcia-Bosch, I.; Company, A.; Costas, M. *Acc. Chem. Res.* **2015**, *48*, 2397–2406.
- (12) For other examples of Cu-based phenolate oxygenations, see: (a) Capdevielle, P.; Maumy, M. *Tetrahedron Lett.* **1982**, *23*, 1577–1580. (b) Casella, L.; Gullotti, M.; Radaelli, R.; Di Gennaro, P. J. *Chem. Soc., Chem. Commun.* **1991**, 1611–1612. (c) Casella, L.; Monzani, E.; Gullotti, M.; Cavagnino, D.; Cerina, G.; Santagostini, L.; Ugo, R. *Inorg. Chem.* **1996**, *35*, 7516–7525. (d) Monzani, E.; Quinti, L.; Perotti, A.; Casella, L.; Gullotti, M.; Randaccio, L.; Geremia, S.; Nardin, G.; Faleschini, P.; Tabbi, G. *Inorg. Chem.* **1998**, *37*, 553–562. (e) Cheng, Y.-T.; Chen, H.-L.; Tsai, S.-Y.; Su, C.-C.; Tsang, H.-S.; Kuo, T.-S.; Tsai, Y.-C.; Liao, F.-L.; Wang, S.-L. *Eur. J. Inorg. Chem.* **2004**, *2004*, 2180–2188.
- (13) (a) Itoh, S.; Fukuzumi, S. *Acc. Chem. Res.* **2007**, *40*, 592–600. (b) Osako, T.; Ohkubo, K.; Taki, M.; Tachi, Y.; Fukuzumi, S.; Itoh, S. *J. Am. Chem. Soc.* **2003**, *125*, 11027–11033. (c) Paul, P. P.; Tyeklar, Z.; Jacobson, R. R.; Karlin, K. D. *J. Am. Chem. Soc.* **1991**, *113*, 5322–5332. (d) Kitajima, N.; Koda, T.; Iwata, Y.; Morooka, Y. *J. Am. Chem. Soc.* **1990**, *112*, 8833–8839. (e) Obias, H. V.; Lin, Y.; Murthy, N. N.; Pidcock, E.; Solomon, E. I.; Ralle, M.; Blackburn, N. J.; Neuhold, Y.-M.; Zuberbühler, A. D.; Karlin, K. D. *J. Am. Chem. Soc.* **1998**, *120*, 12960–12961. (f) Halfen, J. A.; Young, V. G.; Tolman, W. B. *Inorg. Chem.* **1998**, *37*, 2102–2103.
- (14) Hamann, J. N.; Rolff, M.; Tuzcek, F. *Dalton Trans.* **2015**, *44*, 3251–3258.
- (15) Kobayashi, S.; Higashimura, H. *Prog. Polym. Sci.* **2003**, *28*, 1015–1048.
- (16) (a) Matoba, Y.; Kumagai, T.; Yamamoto, A.; Yoshitsu, H.; Sugiyama, M. *J. Biol. Chem.* **2006**, *281*, 8981–8990. (b) Solomon, E. I.; Ginsbach, J. W.; Heppner, D. E.; Kieber-Emmons, M. T.; Kjaergaard, C. H.; Smeets, P. J.; Tian, L.; Woertink, J. S. *Faraday Discuss.* **2011**, *148*, 11–39. (c) Goldfeder, M.; Kanteev, M.; Isaschar-Ovdat, S.; Adir, N.; Fishman, A. *Nat. Commun.* **2014**, *5*, 4505.
- (17) (a) Réglier, M.; Jorand, C.; Waegell, B. *J. Chem. Soc., Chem. Commun.* **1990**, 1752–1755. (b) Schottenheim, J.; Fateeva, N.; Thimm, W.; Krahmer, J.; Tuzcek, F. *Z. Anorg. Allg. Chem.* **2013**, *639*, 1491–1497. (c) Hamann, J. N.; Tuzcek, F. *Chem. Commun.* **2014**, *50*, 2298–2300. (d) Wilfer, C.; Liebhäuser, P.; Erdmann, H.; Hoffmann, A.; Herres-Pawlis, S. *Eur. J. Inorg. Chem.* **2015**, *2015*, 494–502. (e) Arnold, A.; Metzinger, R.; Limberg, C. *Chem. - Eur. J.* **2015**, *21*, 1198–1207. (f) Schottenheim, J.; Gernert, C.; Herzigkeit, B.; Krahmer, J.; Tuzcek, F. *Eur. J. Inorg. Chem.* **2015**, *2015*, 3501–3511.
- (18) (a) Mirica, L. M.; Vance, M.; Rudd, D. J.; Hedman, B.; Hodgson, K. O.; Solomon, E. I.; Stack, T. D. P. *J. Am. Chem. Soc.* **2002**, *124*, 9332–9333. (b) Mirica, L. M.; Rudd, D. J.; Vance, M. A.;

Solomon, E. I.; Hodgson, K. O.; Hedman, B.; Stack, T. D. P. *J. Am. Chem. Soc.* **2006**, *128*, 2654–2665.

(19) Verma, P.; Weir, J.; Mirica, L.; Stack, T. D. P. *Inorg. Chem.* **2011**, *50*, 9816–9825.

(20) **4** is not always obtained in bulk reactions that are carried out at concentrations higher than those used in these UV–visible experiments.<sup>4a,c</sup>

(21) Mirica, L. M.; Stack, T. D. P. *Inorg. Chem.* **2005**, *44*, 2131–2133.

(22) See: Hoover, J. M.; Ryland, B. L.; Stahl, S. S. *J. Am. Chem. Soc.* **2013**, *135*, 2357–2367 and refs 32 and 33 therein.

(23) (a) Fujieda, N.; Murata, M.; Yabuta, S.; Ikeda, T.; Shimokawa, C.; Nakamura, Y.; Hata, Y.; Itoh, S. *JBIC, J. Biol. Inorg. Chem.* **2013**, *18*, 19–26. (b) Suzuki, K.; Shimokawa, C.; Morioka, C.; Itoh, S. *Biochemistry* **2008**, *47*, 7108–7115.

(24) Some tyrosinase enzymes<sup>25a,b</sup> or synthetic models<sup>10b</sup> do not exhibit a KIE, while the model system by Herres-Pawlis et al. surprisingly exhibits a noninverse KIE of 1.2(2).<sup>10h</sup> Also, the one example of aromatic hydroxylation in a constrained **P** does not exhibit a KIE.<sup>25c</sup>

(25) (a) Muñoz-Muñoz, J. L.; Berna, J.; García-Molina, M. d. M.; García-Molina, F.; García-Ruiz, P. A.; Varon, R.; Rodríguez-Lopez, J. N.; García-Canovas, F. *Biochem. Biophys. Res. Commun.* **2012**, *424*, 228–233. (b) Morioka, C.; Tachi, Y.; Suzuki, S.; Itoh, S. *J. Am. Chem. Soc.* **2006**, *128*, 6788–6789. (c) Qayyum, M. F.; Sarangi, R.; Fujisawa, K.; Stack, T. D. P.; Karlin, K. D.; Hodgson, K. O.; Hedman, B.; Solomon, E. I. *J. Am. Chem. Soc.* **2013**, *135*, 17417–17431.

(26) Experiments conducted at –115 °C require MeTHF, creating an important difference with our experiments conducted in CH<sub>2</sub>Cl<sub>2</sub> at –78 °C. The extent to which this solvent switch changes the details of *ortho*-oxygenation remains unclear, but we attribute our ability to visualize **P** at –115 °C to a decreased rate of phenolate binding and OAT in a more coordinating and viscous solvent.

(27) Because of the flatness of their UV–visible spectrum, **C** and similar species have not been characterized by resonance Raman spectroscopy.<sup>9,10</sup>

(28) Pierpont, C. G.; Lange, C. W. *Prog. Inorg. Chem.* **2007**, *41*, 331–442.

(29) (a) Marín-Zamora, M. E.; Rojas-Melgarejo, F.; García-Cánovas, F.; García-Ruiz, P. A. *J. Biotechnol.* **2009**, *139*, 163–168. (b) Guazzaroni, M.; Crestini, C.; Saladino, R. *Bioorg. Med. Chem.* **2012**, *20*, 157–166.

(30) Kubas, G. J. *Inorg. Synth.* **1990**, *28*, 68–70.